University of Toulon

Underwater Robotics, Modelling and Control

Modeling and Control of Underwater Vehicle - SPARUS

Author:
Farooq OLANREWAJU
Nimra JABEEN

15th January 2023

Table of Contents

List of Figures ii

List of Tables ii

1 Introduction 1

1.1 Aim . . . 1

1.2 Objectives . . . 1

1.3 Autonomous Underwater Vehicle: Sparus . . . 1

1.4 Dynamic Model of the AUV Sparus . . . 2

2 Model Identification 4

2.1 Introduction . . . 4

2.2 Multibody Analysis . . . 4

2.3 Identification of RigidBody Mass Matrix . . . 4

2.3.1 Computing the Dimensions of Each Body . . . 4

2.3.2 Computing the Mass and Inertia of Each Body . . . 5

2.3.3 Rigid-Body Mass Matrix at Body Centres of the Sparus . . . 9

2.3.4 Global Rigid Body Mass Matrix of the Sparus . . . 10

2.3.5 Comparison of Body-Centred Rigid Body Mass Matrices (at the Centre of the Sparus) to the Total Rigid Body Mass Matrix . . . 11

2.4 Identification of the Added Mass Matrix . . . 12

2.4.1 Added Body Mass Matrix at the Centre of Gravity of Sparus . . . 12

2.4.2 The Global Added Mass Matrix . . . 14

2.4.3 Comparison of Body-Centred Added Mass Matrices (at the Centre of the Sparus) to the Total Added Mass Matrix . . . 14

2.5 Global Mass Matrix . . . 15

2.5.1 Comparison of Body-Centred Global Mass Matrices (at the Centre of the Sparus) to the Total Global Mass Matrix . . . 16

2.6 Drag Modelling . . . 17

2.6.1 Comparing the Friction Matrices with the Friction Matrix of the Main Body 18

2.7 Coriolis Matrix Modelling . . . 19

2.8 Thruster Mapping . . . 19

3 Simulations and Results 20

3.1 Validating the Simulation . . . 20

3.1.1 Checking for the Effect of Buoyancy. Thrusters = [0%, 0%, 0%] . . . 20

3.1.2 When accelerating downwards. Thrusters = [10%, 0%, 0%] . . . 22

3.1.3 Activating only one of the forward thrusters. Thrusters = [0%, 0%, 10%] . 23
3.2 Imposing Linear Accelerations 25
3.2.1 Imposing Linear Acceleration on the X-Axis 25
3.2.2 Imposing Linear Acceleration on the Z-Axis 26

Bibliography **27**

List of Figures

1 Autonomous Underwater Vehicles 2
2 Small division of the Sparus AUV for dimension measurements 5
3 Main Division of the Sparus AUV Body 6
4 XY-trajectory (left) and Depth Trajectory (Right) of the Sparus when the Thrusters applied are [0%, 0%, 0%]. 20
5 Position, Velocity and Acceleration of the Sparus when the Thrusters applied are [0%, 0%, 0%]. 21
6 Position, Velocity and Acceleration of the Sparus when the Thrusters applied are [0%, 0%, 0%]. 21
7 XY-trajectory (left) and Depth Trajectory (Right) of the Sparus when the Thrusters applied are [10%, 0%, 0%]. 22
8 Position, Velocity and Acceleration of the Sparus when the Thrusters applied are [10%, 0%, 0%]. 22
9 Position, Velocity and Acceleration of the Sparus when the Thrusters applied are [10%, 0%, 0%]. 23
10 XY-trajectory (left) and Depth Trajectory (Right) of the Sparus when the Thrusters applied are [0%, 0%, 10%]. 23
11 Position, Velocity and Acceleration of the Sparus when the Thrusters applied are [0%, 0%, 10%]. 24
12 Position, Velocity and Acceleration of the Sparus when the Thrusters applied are [0%, 0%, 10%]. 24
13 Imposing Linear Acceleration on the X-Axis 25
14 Imposing Linear Acceleration on the Z-Axis 26

List of Tables

1 AUV Sparus Specifications 2
2 Measurements and Scalings 5
3 Estimated volume of each bodies 6
4 Mass of Each Sparus Body 7
5 Centre of Mass and Moment of Inertia of the Small Divisions of the Sparus AUV . 8

6 Centre of Mass and Moment of Inertia of Each Sparus Body 9

1 Introduction

1.1 Aim

To develop expertise in underwater robotics by modelling and controlling the Autonomous Underwater Vehicle (AUV) Sparus.

1.2 Objectives

During the course of this project, we expect to meet the following objectives

1. Estimate the mass and inertia of each body by considering a constant density of the vehicle.
2. Compute each mass matrix at the gravity center of the sparus, comparison of the values of the main solid with the others and conclusion.
3. Compute the added mass matrix at the gravity center of the sparus, excepting the main body, the centre of gravity and centre of buoyancy of the other bodies are the same point compute the global added mass matrix and conclude.
4. Estimation of all drag matrices.
5. Complete and validate the simulator of underwater robotics.
6. Investigating the impact of the different coefficients in the global mass matrix.
7. Investigating the impact of the drag forces of the different bodies

1.3 Autonomous Underwater Vehicle: Sparus

Sparus is a lightweight autonomous underwater vehicle for shallow waters depths of up-to $200m$ which is developed by IQUA Robotics. In this section we will discuss the main characteristics of the vehicle, along with its dynamic model.

Description

Sparus is a shallow hovering vehicle which is able to carry configurable payloads and an open software architecture. The vehicle's torpedo design produces excellent performance, extensive endurance, and effective hydrodynamics. Sparus makes an outstanding tool for commercial, scholarly, and scientific applications thanks to its versatility in both software and hardware.

1. Torpedo-shaped for efficient hydrodynamics and better autonomy.
2. Hovering capable, high maneuverability.
3. Lightweight.
4. Easy operation. It can be deployed by 2 people from any boat.
5. Open hardware for easy payload integration.
6. ROS-based software architecture.
7. Low cost.

Figure 1: Autonomous Underwater Vehicles
IQUA-Robotics (2022)

S-No.	Feature	Parameter
1	Length	1.6 m
2	Hull Diameter	0.23 m
3	Max. Width	0.46 m
4	Weight in Air	52 kg
5	Max. Depth	200 m
6	Endurance	8-10 hrs
7	Max Surge Velocity	3 knots

Table 1: AUV Sparus Specifications

Specifications

The AUV Sparus is made of modular aluminum which is depicted in figure 1. The AUV is propelled by up to three thrusters, giving it three degrees of freedom in the surge, heave, and yaw axes. The vehicle's software design employs an adaptable and open motion control system and is based on ROS over Linux Ubuntu. The table1displays the AUV's mechanical specifications.

The AUV's payload consists of a WiFi or Ethernet umbilical communication system. An Ultra-Short Base Line (USBL) acoustic modem, a Doppler Velocity Logger (DVL), an Inertial Measurement Unit (IMU), a depth sensor, and other sensors are on board the AUV for navigation.

1.4 Dynamic Model of the AUV Sparus

In this section we will document the Dynamic model being used for the AUV Sparus.

Reference Frames

The earth-inertial frame $\{n\}$ and the body-fixed frame $\{b\}$ are the two geometric reference frames that we define. The first of the two depicts a frame that is fixed in relation to the reference ellipsoid of Earth, with the x, y, and z axes pointing, respectively, north-east-down. The latter shows a frame that is fastened to the vehicle's center of gravity, with the x, y, and z axes each pointing in the direction of the longitudinal, transverse, and normal axis of the vehicle.

$\vec{\eta}$ and $\vec{v}$, which stand for the position vector in $\{n\}$ and the velocity vector in $\{b\}$, respectively, are the two vectors that define the state of the vehicle. The relationship between the two vectors is established by the generalized transformation matrix theta as follows:

$$\dot{\vec{\eta}} = J_\theta \vec{v} \tag{1}$$

$$\dot{\vec{\eta}} = \begin{bmatrix} \dot{x} & \dot{y} & \dot{z} & \dot{\theta} & \dot{\phi} & \dot{\psi} \end{bmatrix}^T \tag{2}$$

$$\vec{v} = \begin{bmatrix} u & v & w & p & q & r \end{bmatrix}^T \tag{3}$$

$$J_\theta = \begin{bmatrix} R_\theta & 0_{3\times3} \\ 0_{3\times3} & T_\theta \end{bmatrix} \tag{4}$$

where the matrices for rotation and transformation, respectively, are denoted by R_θ and T_θ.

The Generalized Force Vector

The total force operating on the vehicle, as indicated in n $\{b\}$, is represented by the generalized force vector or τ_{RB}. According to Fossen forces acting on the vehicle are Fossen 2011.

$$\tau_{RB} = \tau + \tau_{wind} + \tau_{waves} - D(v)v + g(\eta) \tag{5}$$

where,
τ, τ_{wind}, τ_{waves} are vectors of control input, wind loads and wave loads,
$D(v)v$ and $g(\eta)$ are the forces and moments due to hydrodynamic damping and gravitational/buoyancy.

Friction Forces are a component of the hydrodynamic drag forces that the vehicle is subjected to as a result of moving through the fluid. These are caused by a variety of phenomena, including vortex shedding, skin friction, pressure friction, and others. Assume frictional forces in our situation will take the following form:

$$F_d = D_{NL}|v|v \tag{6}$$

where, v is the velocity of the underwater vehicle and D_{NL} is the non-linear friction term .

Thruster Forces are the thrusters' forces and moments applied to the AUV. The contribution of thruster forces in our model is given by

$$\tau = \sum_{n=1}^{3} E^b \tau_n^b \tag{7}$$

where, E^b is the allocation matrix that transforms the force vector from thruster frame to $\{b\}$.

Linearized 6DOF Rigid Body Equations of Motion

To express the dynamics of the vehicle a simplified model is given by

$$M\dot{v} + C(v)v = \tau + \tau_{wind} + \tau_{waves} - D(v)v + g(\eta) \tag{8}$$

where

$$M = M_{RB} + M_A \rightarrow \text{System inertia matrix}$$

$$C(v) = C_{RB}(v) + C_A(v) \rightarrow \text{Coriolis centripetal matrix}$$

Added Mass indicates the contribution of forces that are applied to the vehicle as a result of the fluid's motion around it. The fluid around the moving vehicle in the water flows with it and generates a force equal to mass times acceleration. Therefore, this force can be thought of as an addition to the object's mass in the fluid. Both the centripetal matrix and the inertia mass are impacted by this term.

2 Model Identification

2.1 Introduction

The AUV's comprehensive dynamic model is highly useful for understanding and forecasting its behavior in a variety of situations. The dynamic model can be used, among other things, to simulate a vehicle and test various controllers that, due to mechanical and environmental restrictions, cannot be done on an actual vehicle. We will talk about the analytical techniques used to determine the Sparus AUV model in this part.

2.2 Multibody Analysis

The SPARUS AUV is made up of many different parts, including a frame, electronic parts, sensors, cables, etc. The model identification is a difficult challenge because each component must be taken into account separately. They have been assembled into sizable entities to examine the AUV's dynamics. **In this report, the bodies that have been analysed are the torpedo shaped body of the AUV (main body), thrusters, sensors on the front of the AUV (USBL) and the antenna. The other sensors such as side-scan sonar and DVL are considered merged with the main body.**The additional mass and drag acting on each body's center of gravity have been calculated using semi-empirical methods and changed in the body fixed frame of the AUV using the required transformations.

2.3 Identification of RigidBody Mass Matrix

To analyze the inertial forces acting on the dynamic system, the estimation of the mass matrix is necessary. Without any boundary effect, the AUV has been regarded as fully submerged. The AUV is subject to inertial forces from two different types of masses. First, the rigid body mass, which is equal to the mass of the car in air assuming no water fills it up when it is submerged. The second is the extra mass, or virtual mass, that the vehicle must move in order to maneuver in the fluid.

2.3.1 Computing the Dimensions of Each Body

In order to compute the dimensions of all bodies we have used a scale and calculated the dimensions by hand. After measuring the dimensions we scaled the measurements to the dimensions given for the Sparus total length and radius.

The Sparus is divided into ten parts for measurements. The total length of the Sparus is 1.6m and the radius of the main body is 0.115m. Hence, the measurements are scaled to attain this values as shown in Table 2. These measurements are used to estimate some properties of the Sparus.

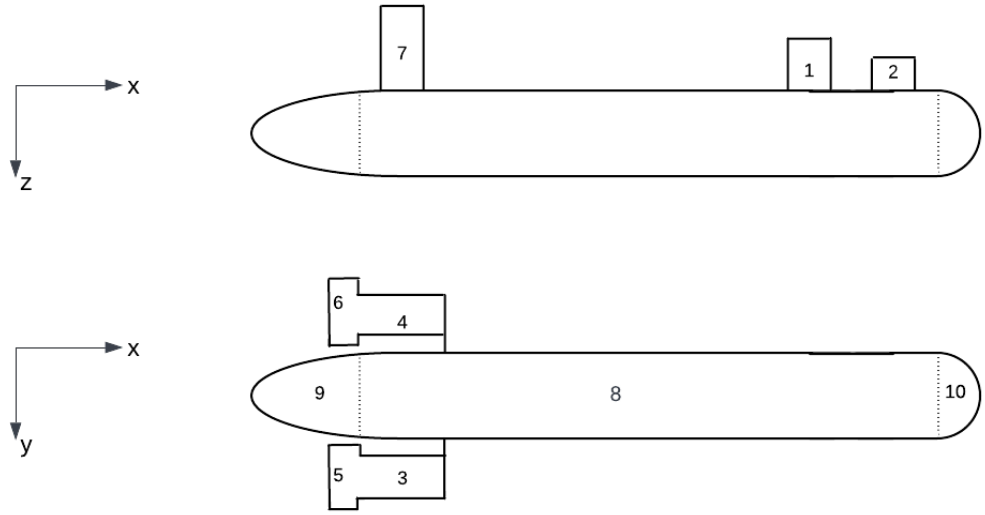

Figure 2: Small division of the Sparus AUV for dimension measurements

ID	Measured Values (cm)	Scaled Values (m)
1	(0.5 0.5 0.2)	(0.0578 0.0575 0.0230)
2	(0.5 0.5 0.2)	(0.0578 0.0575 0.0575)
3	(1.6 0.5 0.5)	(0.1848 0.0575 0.0575)
4	(1.6 0.5 0.5)	(0.1848 0.0575 0.0575)
5	(0.45 0.9 0.9)	(0.0520 0.1035 0.1035)
6	(0.45 0.9 0.9)	(0.0520 0.1035 0.1035)
7	(0.7 0.4 2.2)	(0.0809 0.0575 0.0575)
8	(10.85 2.0 2.0)	(1.2534 0.2300 0.2300)
9	(2.2 2.0 2.0)	(0.2542 0.2300 0.2300)
10	(0.8 2.0 2.0)	(0.0924 0.2300 0.2300)

Table 2: Measurements and Scalings

2.3.2 Computing the Mass and Inertia of Each Body

Firstly, the volume of all bodies according to their shape were calculated. There are seven cylinder bodies, one cuboid, one cone and one hemi-ellipsoid. The values are provided in Table 3

ID	Shape	Volume (m^3)	Mass (kg)
1	Cylinder	$V = \pi \times \frac{0.0578}{2}^2 \times 0.0230 = 6.027e-05$	0.0513
2	Cylinder	$V = \pi \times \frac{0.0578}{2}^2 \times 0.0575 = 1.507e-04$	0.1281
3	Cylinder	$V = \pi \times \frac{0.0575}{2}^2 \times 0.1848 = 4.780e-04$	0.4082
4	Cylinder	$V = \pi \times \frac{0.0575}{2}^2 \times 0.1848 = 4.780e-04$	0.4082
5	Cylinder	$V = \pi \times \frac{0.1035}{2}^2 \times 0.0520 = 4.374e-04$	0.3720
6	Cylinder	$V = \pi \times \frac{0.1035}{2}^2 \times 0.0520 = 4.374e-04$	0.3720
7	Cuboid	$V = 0.0809 \times 0.0575 \times 0.0575 = 9.411e-04$	0.8004
8	Cylinder	$V = \pi \times \frac{0.2300}{2}^2 \times 1.2534 = 0.0521$	44.2894
9	Cone	$V = \frac{\pi}{3} \times \frac{0.2300}{2}^2 \times 0.2542 = 0.0035$	2.9934
10	Hemi-ellipsoid	$V = \frac{2\pi}{3} \times \frac{0.2300}{2}^2 \times 0.0924 = 0.0026$	2.1771

Table 3: Estimated volume of each bodies

$$V_{total} = 0.0611m^3$$

After the total volume was calculated by summing up volumes of all bodies, it was assumed that the density of the Sparus is constant for ease of computation (since the material of each bodies and their densities are unknown). Then, the density is computed in Equation 9 by dividing the total mass ($= 52kg$) by the total volume.

$$\begin{aligned} \rho &= \frac{m_{sparus}}{V_{sparus}} = \frac{52}{0.0611} \\ &= 850.4605kg/m^3 \end{aligned} \tag{9}$$

Hence, the estimated mass of each body is calculated from the volumes and the assumed constant density. The result is also provided in Table 3.

For the main simulation, the Sparus is actually divided into six bodies. The earlier division is only for ease of measurement and volume calculations. The new division

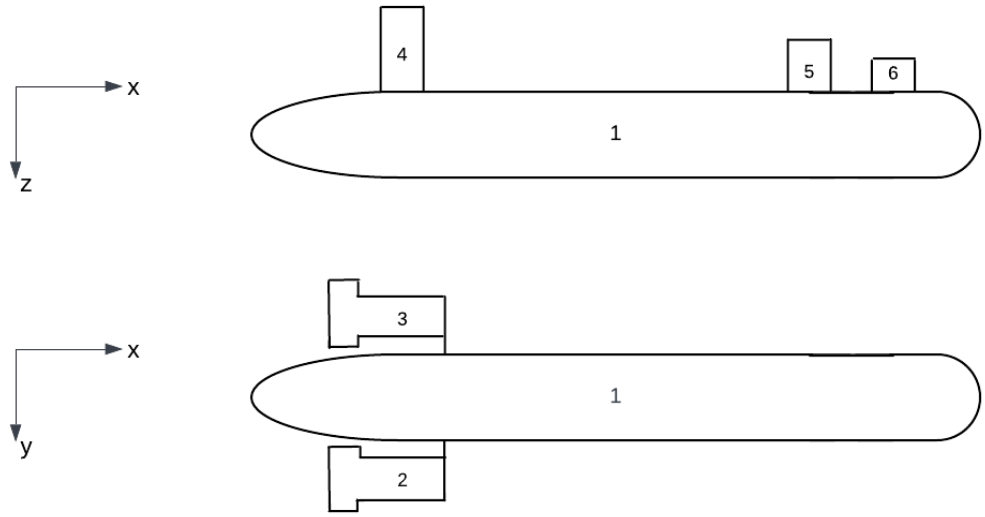

Figure 3: Main Division of the Sparus AUV Body

Hence, the masses of these bodies are calculated from the masses of the smaller divisions.

ID	Mass (kg)
1	$m_1 = 44.2894 + 2.9934 + 2.1771 = 49.4599$
2	$m_2 = 0.4082 + 0.3720 = 0.7802$
3	$m_3 = 0.4082 + 0.3720 = 07802$
4	$m_4 = 0.8004$
5	$m_5 = 0.1281$
6	$m_6 = 0.0513$

Table 4: Mass of Each Sparus Body

Obervation: The mass of the Sparus is concentrated on the main body (i.e. body 1). Among the remaining bodies, the thrusters and the antenna (i.e. bodies 2, 3 and 4) have more considerable masses. While the mass of the remaining two have the least masses.

Before calculating the moment of inertia (MOI) of the six bodies, the centre of mass of each of the small divisions were determined as well as their MoI (see Table 5).

ID	Centre of Mass	Moment of Inertia
1	$\begin{bmatrix} 0.5632 \\ 0 \\ -0.1265 \end{bmatrix}$	$10^{-4}\begin{bmatrix} 0.1295 & 0 & 0 \\ 0 & 0.1295 & 0 \\ 0 & 0 & 0.2138 \end{bmatrix}$
2	$\begin{bmatrix} 0.2975 \\ 0 \\ -0.1438 \end{bmatrix}$	$10^{-4}\begin{bmatrix} 0.3237 & 0 & 0 \\ 0 & 0.3237 & 0 \\ 0 & 0 & 0.5344 \end{bmatrix}$
3	$\begin{bmatrix} -0.6614 \\ 0.2013 \\ 0 \end{bmatrix}$	$\begin{bmatrix} 0.0002 & 0 & 0 \\ 0 & 0.0012 & 0 \\ 0 & 0 & 0.0012 \end{bmatrix}$
4	$\begin{bmatrix} -0.6614 \\ -0.2013 \\ 0 \end{bmatrix}$	$\begin{bmatrix} 0.0002 & 0 & 0 \\ 0 & 0.0012 & 0 \\ 0 & 0 & 0.0012 \end{bmatrix}$
5	$\begin{bmatrix} -0.7798 \\ 0.2013 \\ 0 \end{bmatrix}$	$10^{-3}\begin{bmatrix} 0.4981 & 0 & 0 \\ 0 & 0.0.3328 & 0 \\ 0 & 0 & 0.3328 \end{bmatrix}$
6	$\begin{bmatrix} -0.7798 \\ -0.2013 \\ -0.1438 \end{bmatrix}$	$10^{-3}\begin{bmatrix} 0.4981 & 0 & 0 \\ 0 & 0.3328 & 0 \\ 0 & 0 & 0.3328 \end{bmatrix}$
7	$\begin{bmatrix} -0.5227 \\ 0 \\ -0.2415 \end{bmatrix}$	$\begin{bmatrix} 0.0044 & 0 & 0 \\ 0 & 0.0047 & 0 \\ 0 & 0 & 0.0006 \end{bmatrix}$
8	$\begin{bmatrix} 0 \\ 0 \\ 0 \end{bmatrix}$	$\begin{bmatrix} 0.2929 & 0 & 0 \\ 0 & 5.9450 & 0 \\ 0 & 0 & 5.9450 \end{bmatrix}$
9	$\begin{bmatrix} -0.6903 \\ 0 \\ 0 \end{bmatrix}$	$\begin{bmatrix} 0.0119 & 0 & 0 \\ 0 & 0.0132 & 0 \\ 0 & 0 & 0.0132 \end{bmatrix}$
10	$\begin{bmatrix} 0.6614 \\ 0 \\ 0 \end{bmatrix}$	$\begin{bmatrix} 0.0058 & 0 & 0 \\ 0 & 0.0030 & 0 \\ 0 & 0 & 0.0030 \end{bmatrix}$

Table 5: Centre of Mass and Moment of Inertia of the Small Divisions of the Sparus AUV

Thereafter, the centres of mass of the six bodies were calculated. Then, the MoI of each of the six bodies were determined using parallel axis theorem from the MoI of their smaller divisions.

ID	Centre of Mass	Moment of Inertia
1	$m_1 = 44.2894 + 2.9934 + 2.1771 = 49.4599$	$I_1 = \begin{bmatrix} 0.3105 & 0 & 0 \\ 0 & 8.3396 & 0 \\ 0 & 0 & 8.3396 \end{bmatrix}$
2	$m_2 = 0.4082 + 0.3720 = 0.7802$	$I_2 = \begin{bmatrix} 0.0007 & 0 & 0 \\ 0 & 0.0043 & 0 \\ 0 & 0 & 0.0043 \end{bmatrix}$
3	$m_3 = 0.4082 + 0.3720 = 07802$	$I_3 = \begin{bmatrix} 0.0007 & 0 & 0 \\ 0 & 0.0043 & 0 \\ 0 & 0 & 0.0043 \end{bmatrix}$
4	$m_4 = 0.8004$	$I_4 = \begin{bmatrix} 0.0044 & 0 & 0 \\ 0 & 0.0047 & 0 \\ 0 & 0 & 0.0006 \end{bmatrix}$
5	$m_5 = 0.1281$	$I_5 = 10^{-4} \begin{bmatrix} 0.3237 & 0 & 0 \\ 0 & 0.3237 & 0 \\ 0 & 0 & 0.5344 \end{bmatrix}$
6	$m_6 = 0.0513$	$I_6 = 10^{-4} \begin{bmatrix} 0.1295 & 0 & 0 \\ 0 & 0.1295 & 0 \\ 0 & 0 & 0.2138 \end{bmatrix}$

Table 6: Centre of Mass and Moment of Inertia of Each Sparus Body

Table 6 gives the mass and the MoI of each of the six parts of the Sparus AUV. These MoIs are calculated at the body centres. They would be compared after the values are obtained at the Centre of Gravity of the Sparus.

2.3.3 Rigid-Body Mass Matrix at Body Centres of the Sparus

The mass matrix at the body centre is obtained from the mass m and moment of inertia I_b in Table 6 using Equation 10.

$$M_b^b = \begin{bmatrix} m\mathbf{I}_{3\times3} & \mathbf{0}_{3\times3} \\ \mathbf{0}_{3\times3} & \mathbf{I}_b \end{bmatrix} \tag{10}$$

To calculate the mass matrix for each body at the centre of gravity of the Sparus, the mass matrix of each body is initially calculated at the body centre. Then, a transformation matrix (given in Equation 11) is used to compute the rigid-body mass matrix of each body at the Sparus centre of gravity as shown in Equation 12.

$$H = \begin{bmatrix} \mathbf{I}_{3\times3} & \mathbf{S}^T(\mathbf{R}_b^g) \\ \mathbf{0}_{3\times3} & \mathbf{I}_{3\times3} \end{bmatrix} \tag{11}$$

$$M_b^g = H^T \times M_b^b \times H \tag{12}$$

The mass matrices for the bodies are computed on MATLAB [1] and the outputs are provided in Equations 13 - 18.

[1] The solutions are in the SparusIICalculationsv2.mlx file in the submitted folder.

$$M_{b_1} = \begin{bmatrix} 49.4599 & 0 & 0 & 0 & 0 & 0 \\ 0 & 49.4599 & 0 & 0 & 0 & 0 \\ 0 & 0 & 49.4599 & 0 & 0 & 0 \\ 0 & 0 & 0 & 0.3105 & 0 & 0 \\ 0 & 0 & 0 & 0 & 8.3396 & 0 \\ 0 & 0 & 0 & 0 & 0 & 8.3396 \end{bmatrix} \tag{13}$$

$$M_{b_2} = \begin{bmatrix} 0.7802 & 0 & 0 & 0 & 0 & -0.1570 \\ 0 & 0.7802 & 0 & 0 & 0 & -0.5600 \\ 0 & 0 & 0.7802 & 0.1570 & 0.5600 & 0 \\ 0 & 0 & 0.1570 & 0.0323 & 0.1127 & 0 \\ 0 & 0 & 0.5600 & 0.1127 & 0.4063 & 0 \\ -0.1570 & -0.5600 & 0 & 0 & 0 & 0.4379 \end{bmatrix} \tag{14}$$

$$M_{b_3} = \begin{bmatrix} 0.7802 & 0 & 0 & 0.3237 & 0 & 0.1570 \\ 0 & 0.7802 & 0 & 0 & 0 & -0.5600 \\ 0 & 0 & 0.7802 & -0.1570 & 0.5600 & 0 \\ 0 & 0 & -0.1570 & 0.0323 & -0.1127 & 0 \\ 0 & 0 & 0.5600 & -0.1127 & 0.4063 & 0 \\ 0.1570 & -0.5600 & 0 & 0 & 0 & 0.4379 \end{bmatrix} \tag{15}$$

$$M_{b_4} = \begin{bmatrix} 0.8004 & 0 & 0 & 0 & -0.1933 & 0 \\ 0 & 0.8004 & 0 & 0.1933 & 0 & -0.4184 \\ 0 & 0 & 0.8004 & 0 & 0.4184 & 0 \\ 0 & 0.1933 & 0 & 0.0511 & 0 & -0.1010 \\ -0.1933 & 0 & 0.4184 & 0 & 0.2701 & 0 \\ 0 & -0.4184 & 0 & -0.1010 & 0 & 0.2193 \end{bmatrix} \tag{16}$$

$$M_{b_5} = \begin{bmatrix} 0.1281 & 0 & 0 & 0 & -0.0184 & 0 \\ 0 & 0.1281 & 0 & 0.0184 & 0 & 0.0381 \\ 0 & 0 & 0.1281 & 0 & -0.0381 & 0 \\ 0 & 0.0184 & 0 & 0.0027 & 0 & 0.0055 \\ -0.0184 & 0 & -0.0381 & 0 & 0.0140 & 0 \\ 0 & 0.0381 & 0 & 0.0055 & 0 & 0.0114 \end{bmatrix} \tag{17}$$

$$M_{b_6} = \begin{bmatrix} 0.0513 & 0 & 0 & 0 & -0.0065 & 0 \\ 0 & 0.0513 & 0 & 0.0065 & 0 & 0.0289 \\ 0 & 0 & 0.0513 & 0 & -0.0289 & 0 \\ 0 & 0.0065 & 0 & 0.0008 & 0 & 0.0037 \\ -0.0065 & 0 & -0.0289 & 0 & 0.0171 & 0 \\ 0 & 0.0289 & 0 & 0.0037 & 0 & 0.0163 \end{bmatrix} \tag{18}$$

2.3.4 Global Rigid Body Mass Matrix of the Sparus

The sum of the rigid-body mass matrices of each bodies at the Centre of the Sparus is given in Equation 19.

$$M_b = \begin{bmatrix} 52.0000 & 0 & 0 & 0 & -0.21820 & \\ 0 & 52.0000 & 0 & 0.2182 & 0 & -1.4714 \\ 0 & 0 & 52.0000 & 0 & 1.4714 & 0 \\ 0 & 0.2182 & 0 & 0.4296 & 0 & -0.0919 \\ -0.2182 & 0 & 1.4714 & 0 & 9.4535 & 0 \\ 0 & -1.4714 & 0 & -0.0919 & 0 & 9.4624 \end{bmatrix} \tag{19}$$

Observation This matrix is in the shape of a body that has an XZ symmetry. And checking the shape of the Sparus verifies this observation - the Sparus also has an XZ symmetry.

2.3.5 Comparison of Body-Centred Rigid Body Mass Matrices (at the Centre of the Sparus) to the Total Rigid Body Mass Matrix

The rigid-body mass matrix of each body is compared by dividing them by the computed sum to obtain their percentage composition of the non-zero values.

$$divM_{b_1} = \begin{bmatrix} 95.1152 & 0 & 0 & 0 & 0 & 0 \\ 0 & 95.1152 & 0 & 0 & 0 & 0 \\ 0 & 0 & 95.1152 & 0 & 0 & 0 \\ 0 & 0 & 0 & 72.2707 & 0 & 0 \\ 0 & 0 & 0 & 0 & 88.2180 & 0 \\ 0 & 0 & 0 & 0 & 0 & 88.1346 \end{bmatrix} \tag{20}$$

$$divM_{b_2} = \begin{bmatrix} 3.0006 & 0 & 0 & 0 & 0 & 0 \\ 0 & 3.0006 & 0 & 0 & 0 & 76.1194 \\ 0 & 0 & 3.0006 & 0 & 76.1194 & 0 \\ 0 & 0 & 0 & 15.0197 & 0 & 0 \\ 0 & 0 & 76.1194 & 0 & 8.5960 & 0 \\ 0 & 76.1194 & 0 & 0 & 0 & 9.2558 \end{bmatrix} \tag{21}$$

$$divM_{b_3} = \begin{bmatrix} 3.0006 & 0 & 0 & 0 & 0 & 0 \\ 0 & 3.0006 & 0 & 0 & 0 & 76.1194 \\ 0 & 0 & 3.0006 & 0 & 76.1194 & 0 \\ 0 & 0 & 0 & 15.0197 & 0 & 0 \\ 0 & 0 & 76.1194 & 0 & 8.5960 & 0 \\ 0 & 76.1194 & 0 & 0 & 0 & 9.2558 \end{bmatrix} \tag{22}$$

$$divM_{b_4} = \begin{bmatrix} 1.5392 & 0 & 0 & 0 & 88.5863 & 0 \\ 0 & 1.5392 & 0 & 88.5863 & 0 & 28.4330 \\ 0 & 0 & 1.5392 & 0 & 28.4330 & 0 \\ 0 & 88.5863 & 0 & 11.8918 & 0 & 109.9354 \\ 88.5863 & 0 & 28.4330 & 0 & 2.8569 & 0 \\ 0 & 28.4330 & 0 & 109.9354 & 0 & 2.3173 \end{bmatrix} \tag{23}$$

$$divM_{b_5} = \begin{bmatrix} 0.2464 & 0 & 0 & 0 & 8.4421 & 0 \\ 0 & 0.2464 & 0 & 8.4421 & 0 & -2.5906 \\ 0 & 0 & 0.2464 & 0 & -2.5906 & 0 \\ 0 & 8.4421 & 0 & 0.6239 & 0 & -5.9621 \\ 8.4421 & 0 & -2.5906 & 0 & 0.1483 & 0 \\ 0 & -2.5906 & 0 & -5.9621 & 0 & 0.1204 \end{bmatrix} \tag{24}$$

$$divM_{b_6} = \begin{bmatrix} 0.0986 & 0 & 0 & 0 & 2.9716 & 0 \\ 0 & 0.0986 & 0 & 2.9716 & 0 & -1.9618 \\ 0 & 0 & 0.0986 & 0 & -1.9618 & 0 \\ 0 & 2.9716 & 0 & 0.1939 & 0 & -3.9732 \\ 2.9716 & 0 & -1.9618 & 0 & 0.1808 & 0 \\ 0 & -1.9618 & 0 & -3.9732 & 0 & 0.1720 \end{bmatrix} \tag{25}$$

Observations

1. The main body does not have cross term. This is because of its symmetry in its axes. The absence of cross-terms implies that the cross terms are caused by other bodies.
2. The main body has the highest contribution on the main diagonal. About 95% for the mass and 88% for the Moment of Inertia.
3. The two thruster have the next highest contribution after the main bodym followed by the WiFi antenna and the two sensors.
4. Some of the cross terms in the WiFi antenna component (i.e. number 4) is more than 100% because it annuls the opposite effect of cross-terms of the two sensors.

2.4 Identification of the Added Mass Matrix

2.4.1 Added Body Mass Matrix at the Centre of Gravity of Sparus

The added mass matrix is calculated using both the Slender-Body Theorem and the Spheroidal Theorem. These theorems are approximations because it is very difficult and highly computational intensive to compute the added mass numerically. We use the slenderbody theory majorly. And we supplement slenderbody theory with the spheroidal approximation theory where it is impossible to use the slenderbody theory.

For the bodies that the slenderbody approximation could be implemented horizontally such as the main body and the two thrusters, we calculated all the values of the added mass matrix except the first column using the slenderbody approximation. The value at the 1st row and 1st column is computed using Spheroidal approximation. After these values are obtained, the results are trasformed to the Sparus centre and are thus provided in Equations 26-28 [2].

$$M_{a_1} = \begin{bmatrix} 0.5105 & 0 & 0 & 0 & 0 & 0 \\ 0 & 58.4241 & 0 & 0 & 0 & -0.5528 \\ 0 & 0 & 63.7571 & 0 & 3.4022 & 0 \\ 0 & 0 & 0 & 4.2023 & 0 & 0 \\ 0 & 0 & 3.4022 & 0 & 11.2886 & 0 \\ 0 & -0.5528 & 0 & 0 & 0 & 9.7510 \end{bmatrix} \tag{26}$$

[2] All of these are implemented on MATLAB in the SparusIICalculationv2.mlx file.

$$M_{a_2} = \begin{bmatrix} 0.0744 & 0 & 0 & 0 & 0 & -0.0150 \\ 0 & 0 & 0 & 0 & 0 & 0 \\ 0 & 0 & 0 & 0 & 0 & 0 \\ 0 & 0 & 0 & 0 & 0 & 0 \\ 0 & 0 & 0 & 0 & 0 & 0 \\ -0.0150 & 0 & 0 & 0 & 0 & 0.0030 \end{bmatrix} \tag{27}$$

$$M_{a_3} = \begin{bmatrix} 0.0744 & 0 & 0 & 0 & 0 & 0.0150 \\ 0 & 0 & 0 & 0 & 0 & 0 \\ 0 & 0 & 0 & 0 & 0 & 0 \\ 0 & 0 & 0 & 0 & 0 & 0 \\ 0 & 0 & 0 & 0 & 0 & 0 \\ 0.0150 & 0 & 0 & 0 & 0 & 0.0030 \end{bmatrix} \tag{28}$$

N.B.: Since the added mass of the two thrusters are included in the consideration of the main body, the main body was analysed as a cylinder with a fins. Hence, the values for the thrusters given in Equations 27 and 28 are only obtained from Spheroidal approximations.

For the bodies that the slenderbody approximation could be implemented vertically such as the WiFI antenna and the two sensors, we calculated all the values of the added mass matrix except the third column using the slenderbody approximation. The value at the 3rd row and 3rd column is computed using Spheroidal approximation. After these values are obtained, the results are trasformed to the Sparus centre and are thus provided in Equations 30-32 [3]. We derived the formula used as given in Equation 29

$$M_a = \begin{bmatrix} a_{11} & 0 & - & 0 & a_{11}z & 0 \\ 0 & a_{22} & - & -a_{22}z & 0 & 0 \\ - & - & - & - & - & - \\ 0 & -a_{22}z & - & -a_{22}z^2 & 0 & 0 \\ -a_{11}z & 0 & - & 0 & a_{11}z^2 & 0 \\ 0 & 0 & - & 0 & 0 & a_{66} \end{bmatrix} \tag{29}$$

$$M_{a_4} = \begin{bmatrix} -0.7148 & 0 & 0 & 0 & 0.1726 & 0 \\ 0 & -1.7672 & 0 & -0.4268 & 0 & 0.9237 \\ 0 & 0 & 0.0317 & 0 & 0.0166 & 0 \\ 0 & -0.4268 & 0 & -0.1125 & 0 & 0.2231 \\ 0.1726 & 0 & 0.0166 & 0 & -0.0368 & 0 \\ 0 & 0.9237 & 0 & 0.2231 & 0 & -0.4832 \end{bmatrix} \tag{30}$$

$$M_{a_5} = \begin{bmatrix} 0.5226 & 0 & 0 & 0 & -0.0977 & 0 \\ 0 & 0.5226 & 0 & 0.0977 & 0 & 0.1555 \\ 0 & 0 & 0.0184 & 0 & -0.0055 & 0 \\ 0 & 0.0977 & 0 & 0.0200 & 0 & 0.0291 \\ -0.0977 & 0 & -0.0055 & 0 & 0.0216 & 0 \\ 0 & 0.1555 & 0 & 0.0291 & 0 & 0.0462 \end{bmatrix} \tag{31}$$

[3] All of these are implemented on MATLAB in the SparusIICalculationv2.mlx file.

$$M_{a_6} = \begin{bmatrix} 0.3882 & 0 & 0 & 0 & -0.0692 & 0 \\ 0 & 0.3882 & 0 & 0.0692 & 0 & 0.2186 \\ 0 & 0 & 0.0161 & 0 & -0.0091 & 0 \\ 0 & 0.0692 & 0 & 0.0131 & 0 & 0.0390 \\ -0.0692 & 0 & -0.0091 & 0 & 0.0182 & 0 \\ 0 & 0.2186 & 0 & 0.0390 & 0 & 0.1231 \end{bmatrix} \tag{32}$$

2.4.2 The Global Added Mass Matrix

The sum of the all the added mass matrices at the centre of the Sparus gives the Total Added Mass Matrix as provided in Equation 33. This matrix is also in the shape of a matrix with XZ symmetry - which is the symmwtery seen in the Sparus.

$$M_a = \begin{bmatrix} 2.2848 & 0 & 0 & 0 & -0.3395 & 0 \\ 0 & 61.1021 & 0 & 0.5936 & 0 & -1.1025 \\ 0 & 0 & 63.8233 & 0 & 3.4043 & 0 \\ 0 & 0.5936 & 0 & 4.3478 & 0 & -0.1551 \\ -0.3395 & 0 & 3.4043 & 0 & 11.3826 & 0 \\ 0 & -1.1025 & 0 & -0.1551 & 0 & 10.4096 \end{bmatrix} \tag{33}$$

2.4.3 Comparison of Body-Centred Added Mass Matrices (at the Centre of the Sparus) to the Total Added Mass Matrix

The added mass matrix of each body is compared by dividing them by the computed sum to obtain their percentage composition of the non-zero values.

$$divM_{a_1} = \begin{bmatrix} 22.3431 & 0 & 0 & 0 & 0 & 0 \\ 0 & 95.6172 & 0 & 0 & 0 & 50.1433 \\ 0 & 0 & 99.8963 & 0 & 99.9389 & 0 \\ 0 & 0 & 0 & 96.6520 & 0 & 0 \\ 0 & 0 & 99.9389 & 0 & 99.1745 & 0 \\ 0 & 50.1433 & 0 & 0 & 0 & 93.6734 \end{bmatrix} \tag{34}$$

$$divM_{a_2} = \begin{bmatrix} 6.5099 & 0 & 0 & 0 & 0 & 0 \\ 0 & 0 & 0 & 0 & 0 & 0 \\ 0 & 0 & 0 & 0 & 0 & 0 \\ 0 & 0 & 0 & 0 & 0 & 0 \\ 0 & 0 & 0 & 0 & 0 & 0 \\ 0 & 0 & 0 & 0 & 0 & 0.0579 \end{bmatrix} \tag{35}$$

$$divM_{a_3} = \begin{bmatrix} 6.5099 & 0 & 0 & 0 & 0 & 0 \\ 0 & 0 & 0 & 0 & 0 & 0 \\ 0 & 0 & 0 & 0 & 0 & 0 \\ 0 & 0 & 0 & 0 & 0 & 0 \\ 0 & 0 & 0 & 0 & 0 & 0 \\ 0 & 0 & 0 & 0 & 0 & 0.0579 \end{bmatrix} \tag{36}$$

$$divM_{a_4} = \begin{bmatrix} 31.2840 & 0 & 0 & 0 & 50.8488 & 0 \\ 0 & 2.8922 & 0 & 71.8923 & 0 & 83.7886 \\ 0 & 0 & 0.0497 & 0 & 0.4874 & 0 \\ 0 & 71.8923 & 0 & 2.5873 & 0 & 143.8676 \\ 50.8488 & 0 & 0.4874 & 0 & 0.4759 & 0 \\ 0 & 83.7886 & 0 & 143.8676 & 0 & 4.6416 \end{bmatrix} \tag{37}$$

$$divM_{a_5} = \begin{bmatrix} 22.8722 & 0 & 0 & 0 & 28.7674 & 0 \\ 0 & 0.8553 & 0 & 16.4510 & 0 & -14.1008 \\ 0 & 0 & 0.0288 & 0 & -0.1604 & 0 \\ 0 & 16.4510 & 0 & 0.4603 & 0 & -18.7351 \\ 28.7674 & 0 & -0.1604 & 0 & 0.1901 & 0 \\ 0 & -14.1008 & 0 & -18.7351 & 0 & 0.4442 \end{bmatrix} \tag{38}$$

$$divM_{a_6} = \begin{bmatrix} 16.9908 & 0 & 0 & 0 & 20.3838 & 0 \\ 0 & 0.6353 & 0 & 11.6567 & 0 & -19.8311 \\ 0 & 0 & 0.0252 & 0 & -0.2659 & 0 \\ 0 & 11.6567 & 0 & 0.3003 & 0 & -25.1325 \\ 20.3838 & 0 & -0.2659 & 0 & 0.1595 & 0 \\ 0 & -19.8311 & 0 & -25.1325 & 0 & 1.1828 \end{bmatrix} \tag{39}$$

Observations

1. The main body has the highest percentages on the diagonal. It accounts for almost more than 95% except for the value obtained through spheroidal approximations.
2. The main body and thr thrusters have less than 40% contribution in total for the added mass in the position a_{11} (the force component in the X direction due to the acceleration in X). This result is apparently incorrect. And this could be because the value for a_{11} is computed using Slenderbody theory for bodies 4-6 and it was computed using spheroidal approximation for bodies 1-3.
3. The antenna has a higher added mass contribution than the two sensors.

2.5 Global Mass Matrix

The rigid body mass matrix and the added mass matrix about the center of gravity are added to create the global mass matrix. After the summation the global mass matrix of the Sparus at its centre is provided in Equation 40.

$$M_g = \begin{bmatrix} 54.2848 & 0 & 0 & 0 & -0.5577 & 0 \\ 0 & 113.1021 & 0 & 0.8118 & 0 & -2.5739 \\ 0 & 0 & 115.8233 & 0 & 4.8757 & 0 \\ 0 & 0.8118 & 0 & 4.7775 & 0 & -0.2470 \\ -0.5577 & 0 & 4.8757 & 0 & 20.8360 & 0 \\ 0 & -2.5739 & 0 & -0.2470 & 0 & 19.8720 \end{bmatrix} \tag{40}$$

Observations:

1. Acceleration in X-direction causes a moment in Y (due to the $a_{51}term$). And an angular rate in Y will cause an acceleration in X (due to the $a_{15}term$).

2. Likewise, acceleration in Z will also cause a rotation in Y (due to the $a_{53}term$) and vice versa.

These two observations will be checked using the Simulation.

2.5.1 Comparison of Body-Centred Global Mass Matrices (at the Centre of the Sparus) to the Total Global Mass Matrix

The global mass matrix of each body is compared by dividing them by the computed sum to obtain their percentage composition of the non-zero values.

$$divM_{g_1} = \begin{bmatrix} 92.0522 & 0 & 0 & 0 & 0 & 0 \\ 0 & 95.3864 & 0 & 0 & 0 & 21.4776 \\ 0 & 0 & 97.7498 & 0 & 69.7786 & 0 \\ 0 & 0 & 0 & 94.4594 & 0 & 0 \\ 0 & 0 & 69.7786 & 0 & 94.2034 & 0 \\ 0 & 21.4776 & 0 & 0 & 0 & 91.0360 \end{bmatrix} \tag{41}$$

$$divM_{g_2} = \begin{bmatrix} 3.1483 & 0 & 0 & 0 & 0 & 0 \\ 0 & 1.3796 & 0 & 0 & 0 & 43.5156 \\ 0 & 0 & 1.3472 & 0 & 22.9719 & 0 \\ 0 & 0 & 0 & 1.3507 & 0 & 0 \\ 0 & 0 & 22.9719 & 0 & 3.9001 & 0 \\ 0 & 43.5156 & 0 & 0 & 0 & 4.4376 \end{bmatrix} \tag{42}$$

$$divM_{g_3} = \begin{bmatrix} 3.1483 & 0 & 0 & 0 & 0 & 0 \\ 0 & 1.3796 & 0 & 0 & 0 & 43.5156 \\ 0 & 0 & 1.3472 & 0 & 22.9719 & 0 \\ 0 & 0 & 0 & 1.3507 & 0 & 0 \\ 0 & 0 & 22.9719 & 0 & 3.9001 & 0 \\ 0 & 43.5156 & 0 & 0 & 0 & 4.4376 \end{bmatrix} \tag{43}$$

$$divM_{g_4} = \begin{bmatrix} 2.7912 & 0 & 0 & 0 & 65.6141 & 0 \\ 0 & 2.2702 & 0 & 76.3792 & 0 & 52.1431 \\ 0 & 0 & 0.7184 & 0 & 8.9210 & 0 \\ 0 & 76.3792 & 0 & 3.4241 & 0 & 131.2401 \\ 65.6141 & 0 & 8.9210 & 0 & 1.5562 & 0 \\ 0 & 52.1431 & 0 & 131.2401 & 0 & 3.5348 \end{bmatrix} \tag{44}$$

$$divM_{g_5} = \begin{bmatrix} 1.1987 & 0 & 0 & 0 & 20.8149 & 0 \\ 0 & 0.5753 & 0 & 14.2984 & 0 & -7.5207 \\ 0 & 0 & 0.1265 & 0 & -0.8938 & 0 \\ 0 & 14.2984 & 0 & 0.4750 & 0 & -13.9818 \\ 20.8149 & 0 & -0.8938 & 0 & 0.1711 & 0 \\ 0 & -7.5207 & 0 & -13.9818 & 0 & 0.2900 \end{bmatrix} \tag{45}$$

$$divM_{g_6} = \begin{bmatrix} 0.8096 & 0 & 0 & 0 & 13.5710 & 0 \\ 0 & 0.3886 & 0 & 9.3224 & 0 & -9.6156 \\ 0 & 0 & 0.0581 & 0 & -0.7777 & 0 \\ 0 & 9.3224 & 0 & 0.2908 & 0 & -17.2583 \\ 13.5710 & 0 & -0.7777 & 0 & 0.1692 & 0 \\ 0 & -9.6156 & 0 & -17.2583 & 0 & 0.7015 \end{bmatrix} \tag{46}$$

Observations:

1. On the diagonal, the main solid has more than 90% contribution. Followed by the thrusters and the antenna. The two sensors have the least contribution. Hence, the diagonal terms can be modelled by neglecting the sensors.
2. The antenna has the major contribution for the cross terms. It has more than 50% in most cases. Hence, it cannot be neglected since it has a huge impact on the dynamics of the Sparus.
3. The two sensor have about 10% contributions or more in the cross terms (although these are counteracted majorly by the antenna). These values are not insignificant. Hence, it could not be neglected in the dynamics.

2.6 Drag Modelling

The drag matrices are modelled using the same principles as the added mass matrices. These matrices would be used in the Simulator to compute the drag forces acting at different points on the Sparus. Then, the values would be eventually transformed to the centre of the Sparus. The drag matrix for the six bodies are given in Equations 47-52.

$$K_1 = \begin{bmatrix} 4.1548 & 0 & 0 & 0 & 0 & 0 \\ 0 & 55.2000 & 0 & 0 & 0 & 0 \\ 0 & 0 & 55.2000 & 0 & 0 & 0 \\ 0 & 0 & 0 & 0 & 0 & 0 \\ 0 & 0 & 0 & 0 & 7.0656 & 0 \\ 0 & 0 & 0 & 0 & 0 & 7.0656 \end{bmatrix} \tag{47}$$

$$K_2 = \begin{bmatrix} 0.5193 & 0 & 0 & 0 & 0 & 0 \\ 0 & 2.0426 & 0 & 0 & 0 & 0 \\ 0 & 0 & 2.0426 & 0 & 0 & 0 \\ 0 & 0 & 0 & 0 & 0 & 0 \\ 0 & 0 & 0 & 0 & 0.0008 & 0 \\ 0 & 0 & 0 & 0 & 0 & 0.0008 \end{bmatrix} \tag{48}$$

$$K_3 = \begin{bmatrix} 0.5193 & 0 & 0 & 0 & 0 & 0 \\ 0 & 2.0426 & 0 & 0 & 0 & 0 \\ 0 & 0 & 2.0426 & 0 & 0 & 0 \\ 0 & 0 & 0 & 0 & 0 & 0 \\ 0 & 0 & 0 & 0 & 0.0008 & 0 \\ 0 & 0 & 0 & 0 & 0 & 0.0008 \end{bmatrix} \tag{49}$$

$$K_4 = \begin{bmatrix} 6.9828 & 0 & 0 & 0 & 0 & 0 \\ 0 & 12.2755 & 0 & 0 & 0 & 0 \\ 0 & 0 & 1.9529 & 0 & 0 & 0 \\ 0 & 0 & 0 & 0.0035 & 0 & 0 \\ 0 & 0 & 0 & 0 & 0.0080 & 0 \\ 0 & 0 & 0 & 0 & 0 & 0 \end{bmatrix} \tag{50}$$

$$K_5 = \begin{bmatrix} 0.1984 & 0 & 0 & 0 & 0 & 0 \\ 0 & 0.1993 & 0 & 0 & 0 & 0 \\ 0 & 0 & 1.4347 & 0 & 0 & 0 \\ 0 & 0 & 0 & 0.0000 & 0 & 0 \\ 0 & 0 & 0 & 0 & 0.0000 & 0 \\ 0 & 0 & 0 & 0 & 0 & 0 \end{bmatrix} \tag{51}$$

$$K_6 = \begin{bmatrix} 0.4959 & 0 & 0 & 0 & 0 & 0 \\ 0 & 0.4982 & 0 & 0 & 0 & 0 \\ 0 & 0 & 1.4347 & 0 & 0 & 0 \\ 0 & 0 & 0 & 0.0000 & 0 & 0 \\ 0 & 0 & 0 & 0 & 0.0000 & 0 \\ 0 & 0 & 0 & 0 & 0 & 0 \end{bmatrix} \tag{52}$$

2.6.1 Comparing the Friction Matrices with the Friction Matrix of the Main Body

The comparison would only be done for regions that are calculated using the same theories. The values for the bodies 2-3 are computed using the same theory as the main since they are horizontal. While the bodies 4-6 are computed in a slightly different way becasue they have a vertical orientation.

$$divK_2 = \begin{bmatrix} 12.5000 & 0 & 0 & 0 & 0 & 0 \\ 0 & 3.7004 & 0 & 0 & 0 & 0 \\ 0 & 0 & 3.7004 & 0 & 0 & 0 \\ 0 & 0 & 0 & 0 & 0 & 0 \\ 0 & 0 & 0 & 0 & 0.0120 & 0 \\ 0 & 0 & 0 & 0 & 0 & 0.0120 \end{bmatrix} \tag{53}$$

$$divK_3 = \begin{bmatrix} 12.5000 & 0 & 0 & 0 & 0 & 0 \\ 0 & 3.7004 & 0 & 0 & 0 & 0 \\ 0 & 0 & 3.7004 & 0 & 0 & 0 \\ 0 & 0 & 0 & 0 & 0 & 0 \\ 0 & 0 & 0 & 0 & 0.0120 & 0 \\ 0 & 0 & 0 & 0 & 0 & 0.0120 \end{bmatrix} \tag{54}$$

$$divK_4 = \begin{bmatrix} 168.0676 & 0 & 0 & 0 & 0 & 0 \\ 0 & 22.2383 & 0 & 0 & 0 & 0 \\ 0 & 0 & 3.5379 & 0 & 0 & 0 \\ 0 & 0 & 0 & \text{inf} & 0 & 0 \\ 0 & 0 & 0 & 0 & 0.1125 & 0 \\ 0 & 0 & 0 & 0 & 0 & 0 \end{bmatrix} \tag{55}$$

$$divK_5 = \begin{bmatrix} 4.7746 & 0 & 0 & 0 & 0 & 0 \\ 0 & 0.3610 & 0 & 0 & 0 & 0 \\ 0 & 0 & 2.5991 & 0 & 0 & 0 \\ 0 & 0 & 0 & \text{inf} & 0 & 0 \\ 0 & 0 & 0 & 0 & 0.0000 & 0 \\ 0 & 0 & 0 & 0 & 0 & 0 \end{bmatrix} \tag{56}$$

$$divK_6 = \begin{bmatrix} 11.9366 & 0 & 0 & 0 & 0 & 0 \\ 0 & 0.9025 & 0 & 0 & 0 & 0 \\ 0 & 0 & 2.5991 & 0 & 0 & 0 \\ 0 & 0 & 0 & \text{inf} & 0 & 0 \\ 0 & 0 & 0 & 0 & 0.0000 & 0 \\ 0 & 0 & 0 & 0 & 0 & 0 \end{bmatrix} \tag{57}$$

Observations:

1. The values for the first row and first column of the bodies 4-6 are too high and unrealistic. This must have been due to the differences in theories used.
2. When the thrusters are compared to the main body, they have frictional factors that are about 12% of the values of the main body. Hence, it is not negligible.
3. The Antennas has some considerable frictional factors (the values in the position a_{11} is not considered). Hence, it's frictional co-efficient cannot be neglected.
4. The two sensors have very neglible frictional values. Because they have less than 1% compared to the main body. The value with 2.5% was computed using a different theory, hence cannot really be compared.

2.7 Coriolis Matrix Modelling

The coriolis force is dependent on the velocity of the Sparus. The coriolis matrix C is given in Equation 58.

$$C = \begin{bmatrix} \mathbf{0} & -S(M_{11}v1 + M_{12}v2) \\ -S(M_{11}v1 + M_{12}v2) & -S(M_{21}v1 + M_{22}v2) \end{bmatrix} \tag{58}$$

The values of M_{11}, M_{12} and M_{22} are obtained from the global mass matrices. The values of v_1 and v_2 are gotten from the DVL[4].

2.8 Thruster Mapping

$$EB_F = \begin{bmatrix} 0 & 1 & 1 \\ 0 & 0 & 0 \\ 1 & 0 & 0 \end{bmatrix} \tag{59}$$

$$EB_M = \begin{bmatrix} 0 & 0 & 0 \\ 0 & 0 & 0 \\ 0 & 0.1700 & -0.1700 \end{bmatrix} \tag{60}$$

[4]This is implemented in the RovModel.m file in the SImulation

$$EB = \begin{bmatrix} 0 & 1.0000 & 1.0000 \\ 0 & 0 & 0 \\ 1.0000 & 0 & 0 \\ 0 & 0 & 0 \\ 0 & 0 & 0 \\ 0 & 0.1700 & -0.1700 \end{bmatrix} \tag{61}$$

3 Simulations and Results

3.1 Validating the Simulation

Three simulations are tested to validate the Simulation and check if the outputs are consistent with what was expected from the Mass Matrices.

3.1.1 Checking for the Effect of Buoyancy. Thrusters = [0%, 0%, 0%]

When the three thrusters are dead, the bouyancy force is supposed to act on the Sparus and push it to the water surface.

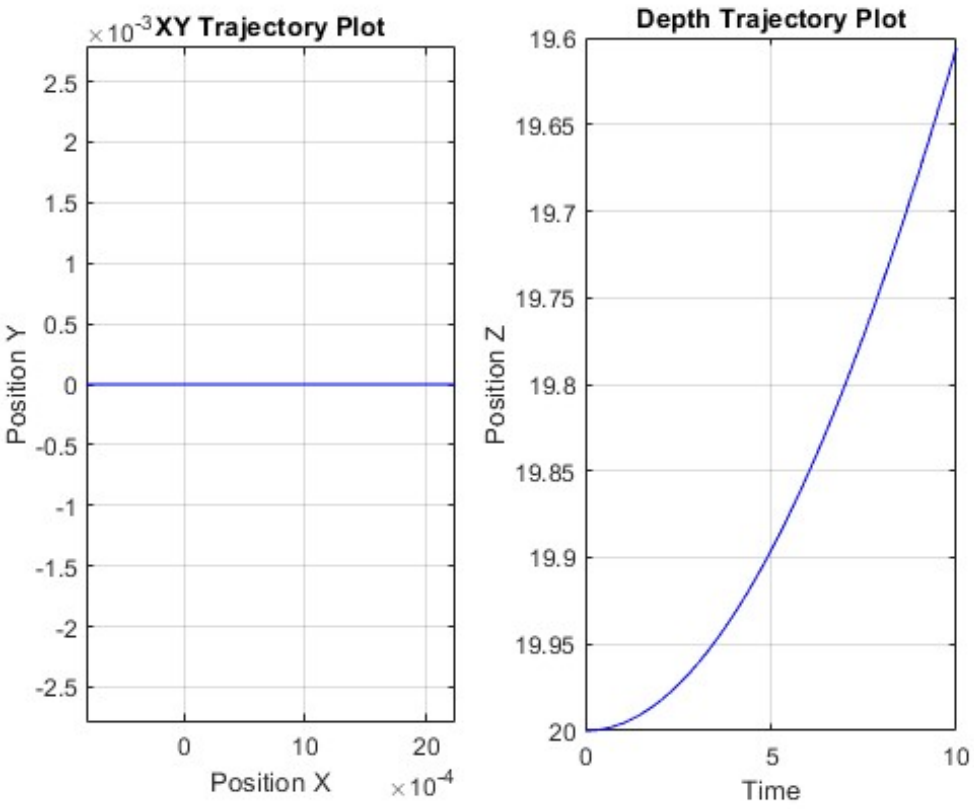

Figure 4: XY-trajectory (left) and Depth Trajectory (Right) of the Sparus when the Thrusters applied are [0%, 0%, 0%].

Observations:

1. As expected, the sparus moves up when all thrusters are dead. Hence, it can be recovered in the case of failure.

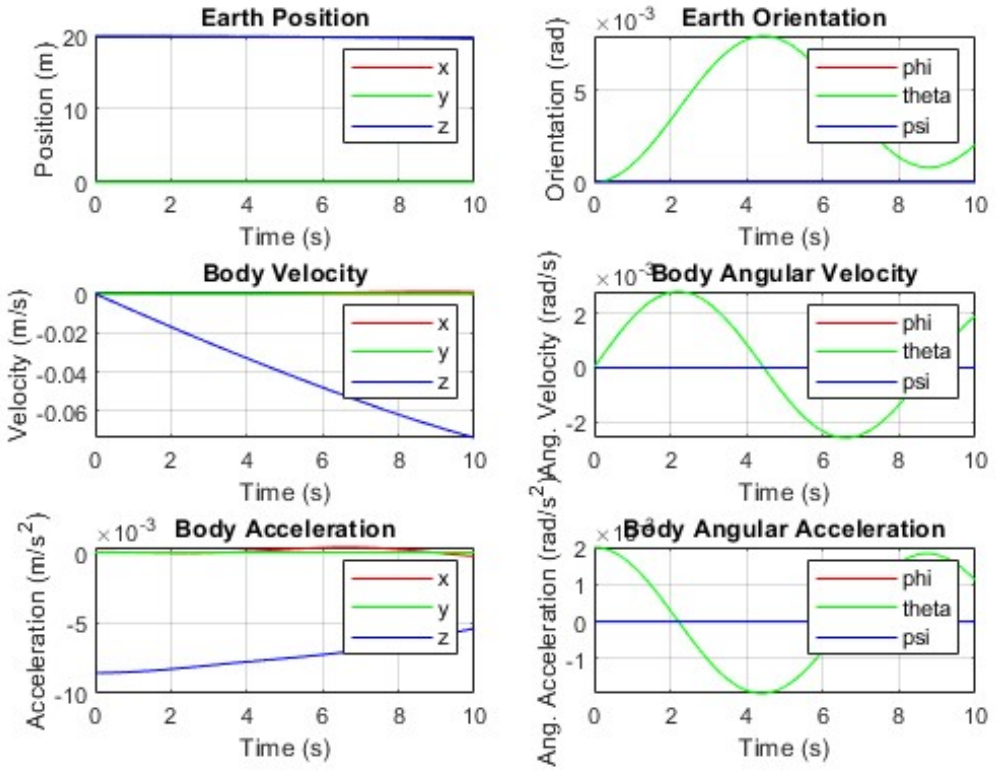

Figure 5: Position, Velocity and Acceleration of the Sparus when the Thrusters applied are [0%, 0%, 0%].

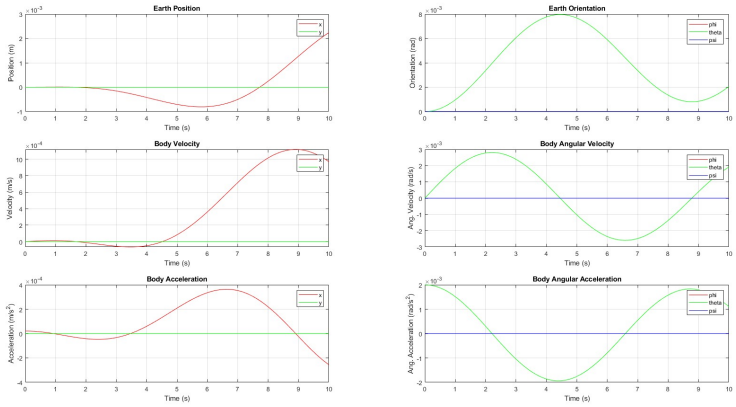

Figure 6: Position, Velocity and Acceleration of the Sparus when the Thrusters applied are [0%, 0%, 0%].

2. According to the global mass matrix, an acceleration in Z will cause a moment in Y. This explains the changes in angle observed in Figure 6 on the top right corner.
3. Conversely, an angular rate in Y will cause an acceleration in X and Z according to the global mass matrix. Hence, this also explains the change in acceleration and velocities in X in Figure 6.
4. It is also suspected that the Coriolis could have effect on the velocity in X. Since the body has a velocity in Z and it is also rotating in Y.

3.1.2 When accelerating downwards. Thrusters = [10%, 0%, 0%]

The dynamics for the downward acceleration is similar to the dynamics for the upwards acceleration except that there is a change in the direction of the angular rate in Y. And this conversely affect the remaining explanations given earlier.

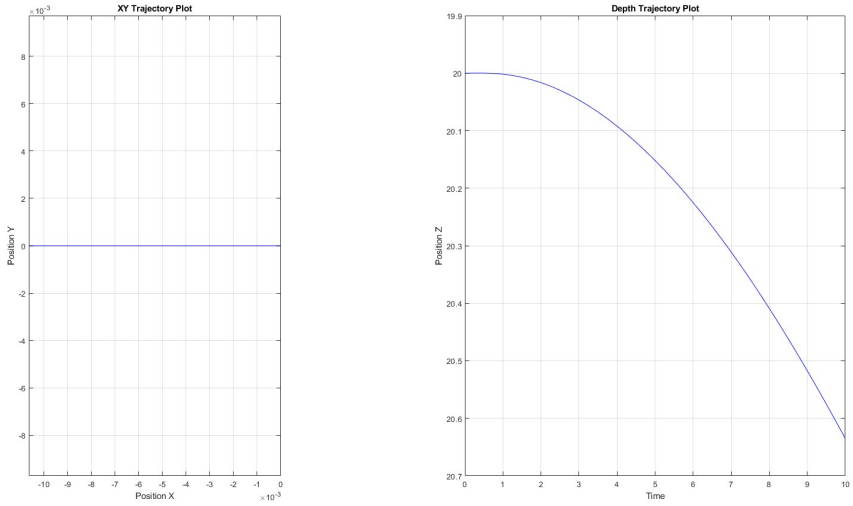

Figure 7: XY-trajectory (left) and Depth Trajectory (Right) of the Sparus when the Thrusters applied are [10%, 0%, 0%].

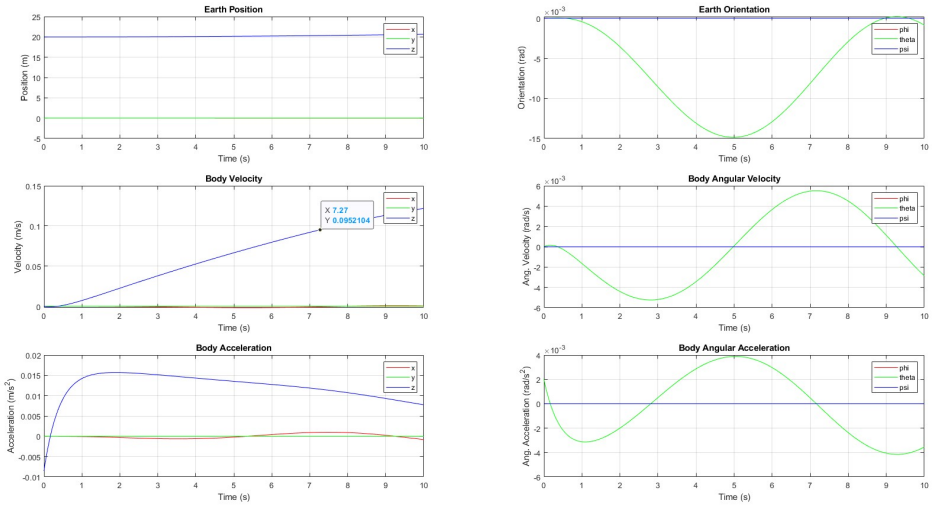

Figure 8: Position, Velocity and Acceleration of the Sparus when the Thrusters applied are [10%, 0%, 0%].

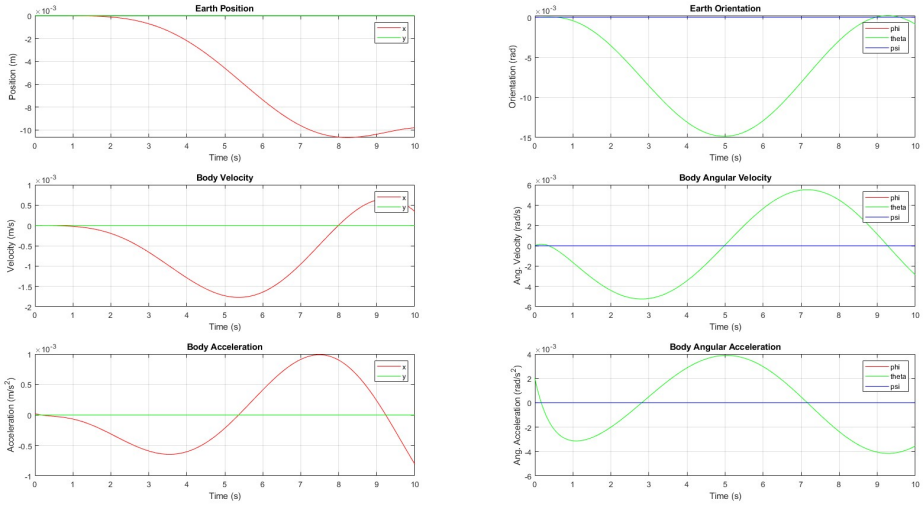

Figure 9: Position, Velocity and Acceleration of the Sparus when the Thrusters applied are [10%, 0%, 0%].

3.1.3 Activating only one of the forward thrusters. Thrusters = [0%, 0%, 10%]

If only one of the forward thrusters is activated, two things are expected:

1. The Sparus should follow a curved path.
2. The coriolis should have more effect because the buoyancy is causing upward forces and the acceleration in the X axis is more pronounced.

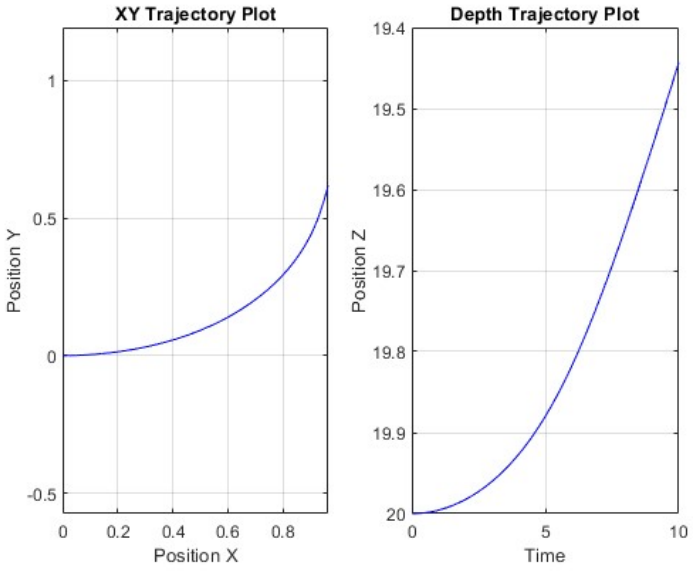

Figure 10: XY-trajectory (left) and Depth Trajectory (Right) of the Sparus when the Thrusters applied are [0%, 0%, 10%].

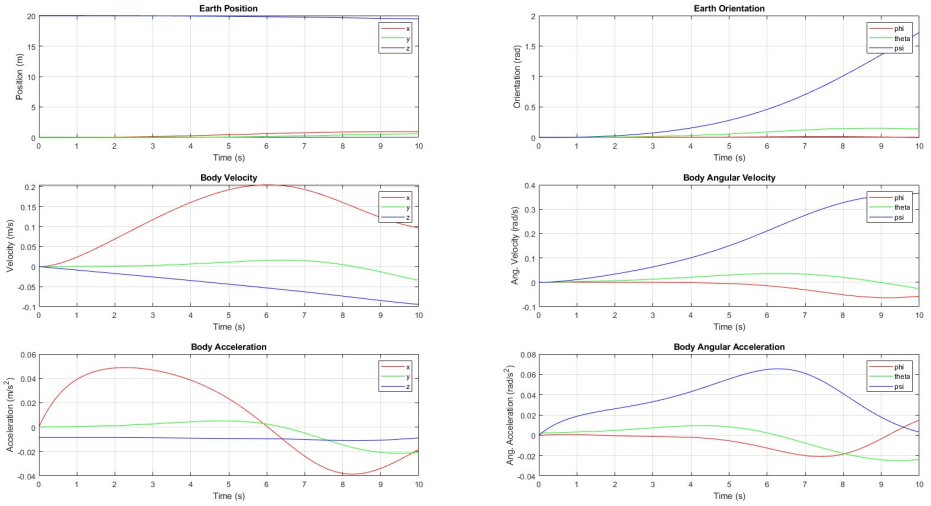

Figure 11: Position, Velocity and Acceleration of the Sparus when the Thrusters applied are [0%, 0%, 10%].

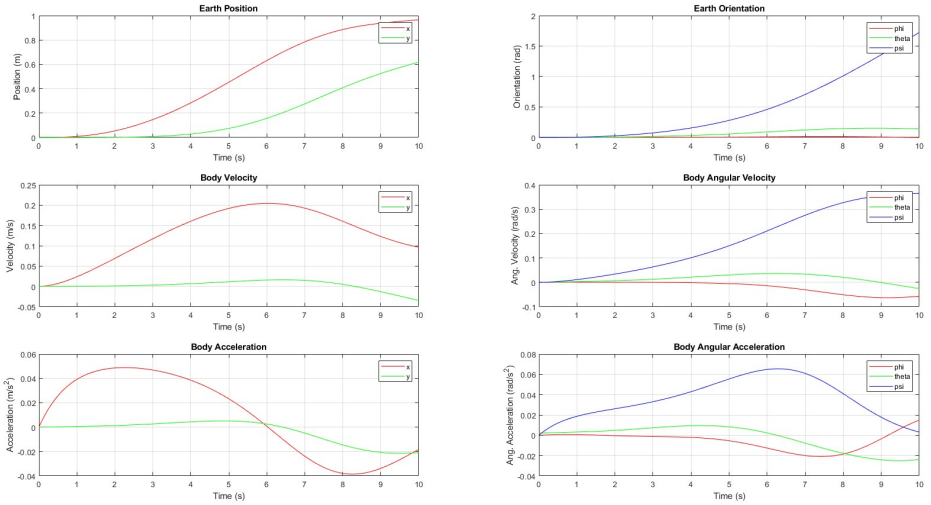

Figure 12: Position, Velocity and Acceleration of the Sparus when the Thrusters applied are [0%, 0%, 10%].

Observations:

1. The Sparus followed a curved path in the XY trajectory due to the effect of the single thruster.
2. The SParus moved towards the surface because the vertical thruster is off.
3. The high angular rate in Z is due to the effect of the moment of the horizontal forces of the thrusters. The force causes a moment because it has a perpendicular distance from the centre of the Sparus.

3.2 Imposing Linear Accelerations

To impose linear acceleration, we assumed that only the thruster forces are acting in the Sparus. This enables us to impose linear acceleration on either the X-axis (by shutting down the vertical thrusters) or the Z-axis (by shutting down the horizontal thrusters).

We are currently unable to verify the cross terms a_{42} and a_{62} because we cannot impose linear accelerations in Y axis.

3.2.1 Imposing Linear Acceleration on the X-Axis

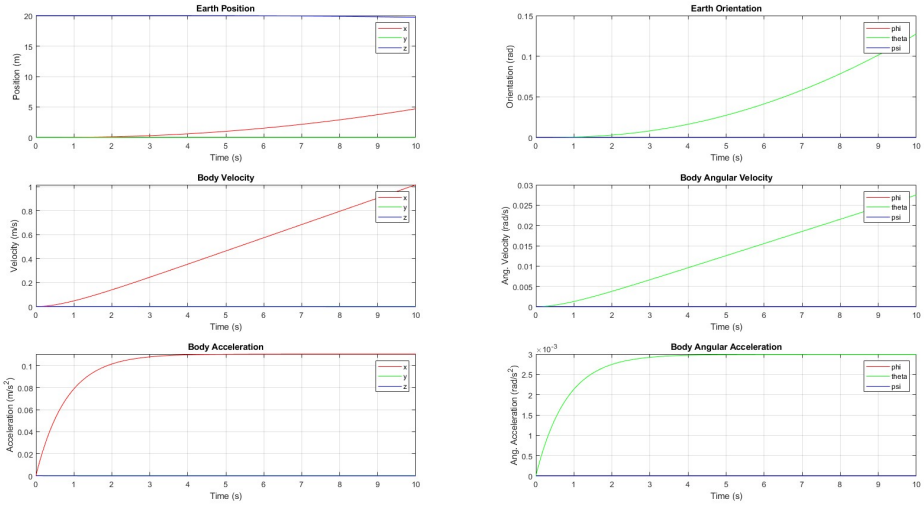

Figure 13: Imposing Linear Acceleration on the X-Axis

Observation:

1. The linear acceleration on X causes an angular rate in Y. This corresponds to the a_{51} component of the global mass matrix.
2.

3.2.2 Imposing Linear Acceleration on the Z-Axis

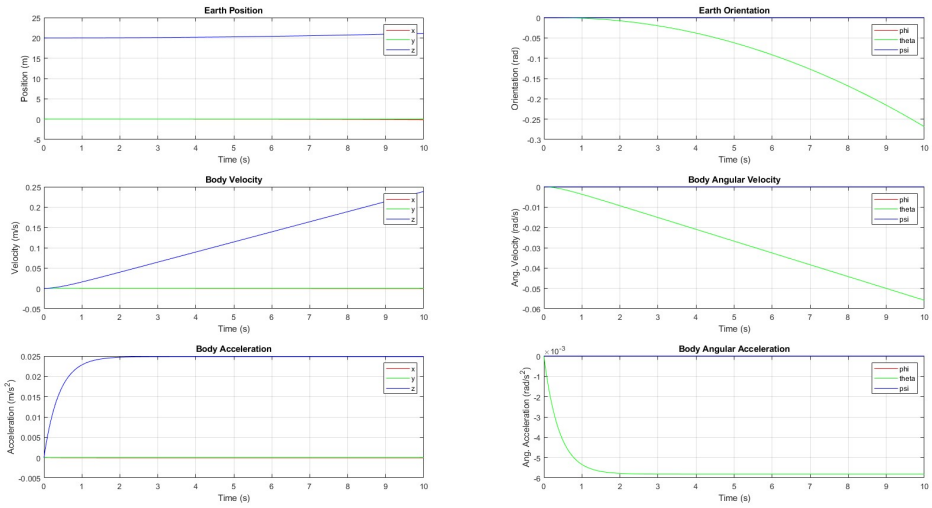

Figure 14: Imposing Linear Acceleration on the Z-Axis

Observation:

1. The linear acceleration on Z causes also causes an angular rate in Y. This corresponds to the a_{53} component of the global mass matrix.

Bibliography

Fossen, Thor I. (Apr. 2011). *Handbook of Marine Craft Hydrodynamics and Motion Control*. John Wiley and Sons. ISBN: 9781119991496. DOI: 10.1002/9781119994138.

IQUA-Robotics (2022). *Sparus II AUV*. URL: https://iquarobotics.com/sparus-ii-auv (visited on 20th Dec. 2022).